

# EFFECT OF LONGITUDINAL RIB SPACING ON DEFORMATION OF ASPHALT PAVEMENT AND FATIGUE OF WELDS IN ORTHOTROPIC STEEL DECK BRIDGE

Iwao SUZUKI\*, Taiichi KAGAYAMA\*\*  
and Masanori IWASAKI\*\*\*

In recent years, fatigue damages both asphalt pavement and welds have been reported in orthotropic steel deck bridge frequently. In order to investigate the effect of longitudinal rib spacing on fatigue damages both asphalt pavement and welds. The large scale model testing which zoom up near main girder web was carried out by using the self-propelled type wheel tracking machine. The spacing between main girder web and longitudinal rib was able to extend in case that through traffic load position is arranged away from main girder web, only the fatigue strength of welds shall be attended.

**Keywords :** *orthotropic steel deck, asphalt pavement, fatigue weld, longitudinal rib, stiffness*

## 1. INTRODUCTION

Due to numerous merits such as the far light weight compared with a concrete slab deck and the short construction period, the orthotropic steel deck bridges have been constructed at many place throughout Japan in the latter half of the 1950s. Recently, it has been used in long span bridges which need to be as light as possible, for example Honshu-Shikoku Bridge and many urban bridges.

While the orthotropic steel deck has the abovementioned merits, it has various problem such as the lack of out-of-plane stiffness due to its light weight, the complex stress behavior, the large stress depending on the structural details and the fatigue cracks due to the direct effect of wheel load.

So many studies have been carried out about the design and construction of the orthotropic steel decks and their asphalt pavements<sup>(1)-(3)</sup>. In particular, a series of studies which carried out centrally by the Public Works Institute in relation to the construction of Honshu-Shikoku Bridge, were compiled into the Design Guidelines for Orthotropic Steel Decks and its Commentary<sup>(4)</sup> (hereinafter referred to as the HSB Design Guidelines). And that has since been used extensively in the design of the orthotropic steel deck bridges.

However, a noticeable increase in recent through-traffic volume, particularly heavy traffic, has accelerated the asphalt pavement deterioration

and the fatigue damages to the details of the orthotropic steel decks, which even now requires further studies<sup>(5)</sup>.

Based on the viewpoints abovementioned, this paper shows the test results using a full-sized model which modify the standard orthotropic steel deck box girder in urban expressway, and the investigation both the wheel load position and the longitudinal rib spacing (main girder web and longitudinal rib spacing) on the deformation of the asphalt pavement laid on the main girder web as well as on the fatigue damages of welds near main girder web.

## 2. REPORTED STUDY RESULTS AND FATIGUE CRACKINGS

For the construction and the fatigue of the orthotropic steel deck bridges, numerous experiments and analysis have been conducted by the quarters involved since this type of bridge was first adopted. Classifying these into (1) structural analysis, (2) asphalt pavement and (3) fatigue, the following can be discussed.

### (1) Results of structural analysis

The analysis methods for the orthotropic steel deck include mainly the theory of orthotropic rectangular plate<sup>(1)</sup>, the finite strip method<sup>(2)</sup> (hereinafter FSM), and the equivalent grille method<sup>(3)</sup>, which are now all generally used as design methods. The finite element method is also used for special structure. There are almost no analytical problem of the design.

### (2) Results of asphalt pavement

The orthotropic steel deck bridges being in existence throughout Japan were investigated by the Public Works Institute in order to clarify the actual conditions of them and the problems (ruts

\* Member of JSCE, Hanshin Expressways Public Corporation (Kyutarocho 4-1-3, Chuoku, Osaka, Japan)

\*\* Member of JSCE, M. Eng., Hanshin Expressway Public Corporation

\*\*\* Member of JSCE, Yokogawa Bridge Works Co., Ltd.

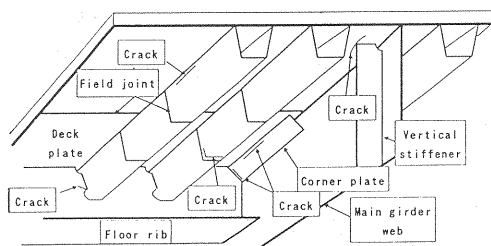


Fig.1 Example of fatigue cracks.

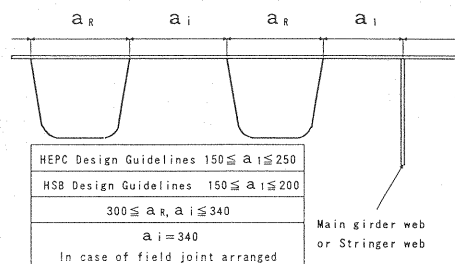


Fig.2 Provisions of longitudinal rib spacing.

and cracks of the asphalt pavement). Along with the investigations, the Institute conducted various experiments and made diverse considerations<sup>8)</sup>. The results are reflected in the provisions of the HSB Design Guidelines, for example the standard floor rib spacing ( $b=2$  m), the standard longitudinal rib spacing, and the standard wheel position (the wheel load shall be not positioned near the stringer beam). In case of urban expressway, it is difficult to satisfy these requirements because of the road alignment, economy and all other reasons, hence the dimensions and the structural details suitable for an individual bridge are employed.

### (3) Results of fatigue

As in a road bridge, the ratio of live load to the design load is small. Therefore, the fatigue has long been regarded as minimal until recent years. But fatigue cracks have been reported in some road bridges<sup>5),9)</sup>. They have occurred in the second structural members due to secondary stress.

The fatigue design method for the orthotropic steel deck has been studied by The Public Works Institute<sup>10)</sup>. This was incorporated in the Specifications for Highway Bridges<sup>11)</sup> as the provisions of the fatigue (the verification for the fatigue by means of a T-load). Also the fatigue verification by the equivalent grille method have been carried out, taking into account an actual state of live load, based on the model of orthotropic steel deck box girder bridge in urban expressway. The requirements for the fatigue design covering specific details are provided<sup>12)</sup>.

For the orthotropic steel decks before introducing the abovementioned provisions for the fatigue, some various type fatigue cracks (See Fig.1) attributable to secondary stresses as in the case of the other steel bridges, have been reported. The fatigue cracks will not lead to the bridge failure. The repairing and/or strengthening them is not easy because the wheel load are directly supported by them. The development of cracks will most probably lead to a decrease in the whole bearing capacity. The consideration of repairing and/or strengthening the fatigue cracks as well as preventing the occurrence of fatigue damage, is urged in

most cases. But the fatigue cracks have occurred in many cases in the structural details of the individual. Then it is necessary to consider the structural details in determining the cause of the fatigue damage, as well as repairing/strengthening method.

When planning how to prevent the fatigue damage by incorporating these facts in the design of a new bridge, it is necessary to consider not only its structural details but also the interrelation between the main girder web and the wheel position, as well as a combination of the asphalt pavement ingredients and so on.

## 3. TESTING METHODS

Longitudinal ribs are divided into two types. First is a closed section rib. Second is a plate type rib. Currently, a U-shaped rib (as per JSS Standards) is applied to urban expressway except for rare case. Longitudinal ribs are arranged generally as shown in Fig.2, where the spacing between the main girder web and its nearest longitudinal rib (hereinafter referred as " $a_I$ ") is an important factor in determining the number of longitudinal ribs in the design, and will greatly affect the workmanship in welding the structural members near the main girder web and in tightening high strength bolts. Narrower spacing is decided in the HSB Design Guidelines, than by the Design Guidelines for Orthotropic Steel Decks issued by the Hanshin Expressway Public Corporation<sup>13)</sup> (hereinafter referred to as the HEPC Design Guidelines).

These provisions abovementioned assume a severer loading condition for the pavement laid on the main girder web on which wheel loads are to travel, thereby providing a greater radius of curvature of the pavement surface. In actual design, however, these provisions embarrass the designer frequently. On the other hand, as according to the past data<sup>14)</sup>, the distribution of vehicles' traveling position on expressway is limited to a considerably confined range. The large distance may be used when the travelling vehicles are positioned far from main girder web. It may

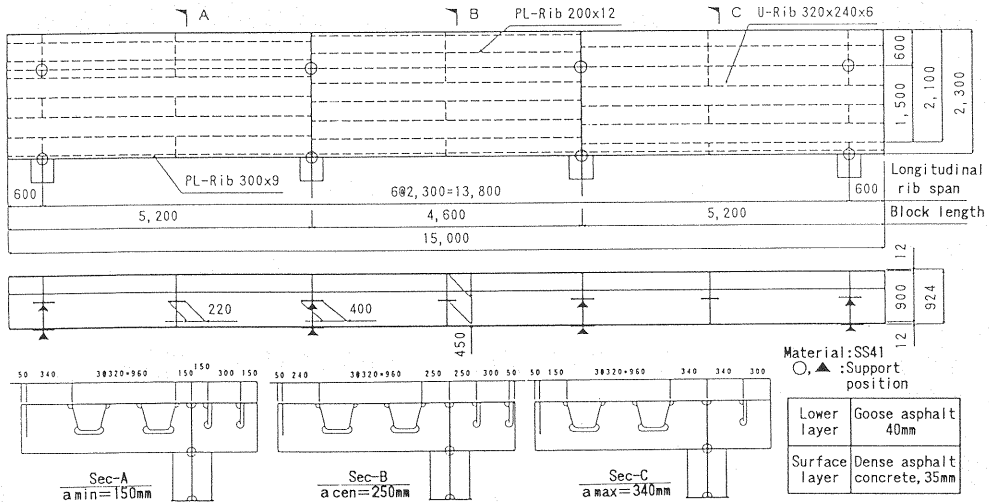


Fig.3 Test model.

well be thought that the allowable range of  $a_1$  can be expanded if the position of traveling vehicles shall be not positioned near the main girder web.

In order to consider both the deformation of asphalt pavement and the fatigue of welds near main girder web, the loading tests shall be carried out. Fig.3 shows the test models which are conducted six spans of longitudinal ribs, they are each provided with supports at the ends of floor ribs.

In the blocks A, B and C, the spacing between the main girder web and longitudinal rib,  $a_1$  includes the following three kinds:

$$a_{\min}=150 \text{ mm}, a_{\text{cen}}=250 \text{ mm}, a_{\max}=340 \text{ mm}$$

$a_{\min}$  and  $a_{\text{cen}}$  are the minimum and the maximum values called for by the HPEC Design Guidelines, and  $a_{\max}$  is a case where the longitudinal rib spacing is greatest when the longitudinal field joints in the deck plate are located nearest the main girder web.

The asphalt pavement was a combination of the standard goose asphalt and the dense asphalt concrete generally used on the urban expressway. The entire width of the test model was paved mechanically at one time.

The Specifications for Highway Bridges stipulate the pavement and the fatigue as follows<sup>15)</sup>:

(1) Longitudinal rib stress due to a T load (not including the impact) shall not exceed the values given in Table 6.2.2.

(2) For the wheel load to be imposed on the orthotropic steel deck, the distribution of load due to the pavement shall not be taken into account.

Therefore, the method of loading suitable for the status quo is preferable when it covers the behaviors of stress in the details, so the most appropriate is the self-propelled type wheel tracking testing machine<sup>16)</sup> capable of applying the

Table 1 Self-propelled type wheel tracking machine.

Property	Load capacity	3.0~25.0 (ton)
	Constant running speed	0.4~5.0 (km/h)
	Machine dead load	2.5 (ton)
	Entire width	1,300 (mm)
	Total running length	14,250 (mm)
Wheel	Size	10.00-20 14PRx2
	Max. allowable load	11 (ton, 7kg/cm <sup>2</sup> )

required load with a double wheel similar to the rear wheel of a heavy-weight vehicle equivalent to a T-20 load. Table 1 shows the capacity of the testing machine and the double wheel.

In order to minimize the effect of temperature variation, static loading tests were applied continuously over a period of time with a minimum of change in outside air temperature, at seven lines in the cross direction (the distance between the main girder web and the wheel position,  $L=0, 150, 250, 350, 450, 600$  and  $850$  mm).

Furthermore, following the completion of static loading tests, repeated loading, at a rate of approx. 5 000 cycles/day, a total of approx. 100 000 cycles, was applied at  $L=850$  mm and  $L=0$  mm, in order to investigate the deforming behavior of the asphalt pavement.

#### 4. EFFECTS OF WHEEL LOAD POSITION AND LONGITUDINAL RIB ARRANGEMENT ON THE PAVEMENT DIRECTLY OVER THE MAIN GIRDER WEB

Fig.4 shows the effect of the wheel positions on the strain of the top surface of the deck plate laid over the main girder web at the center of the longitudinal rib span when being applied with 8

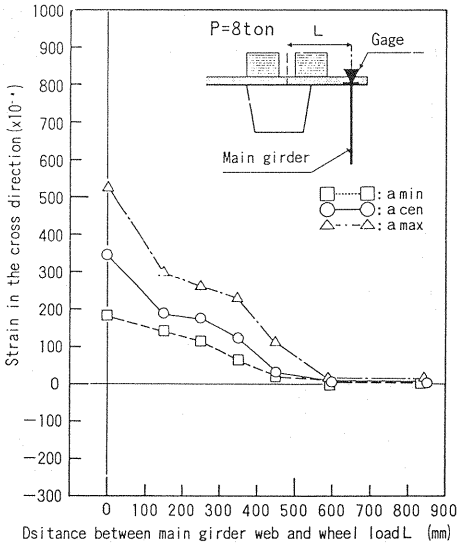


Fig.4 Effect of wheel position on the strain of the top surface of the deck plate.

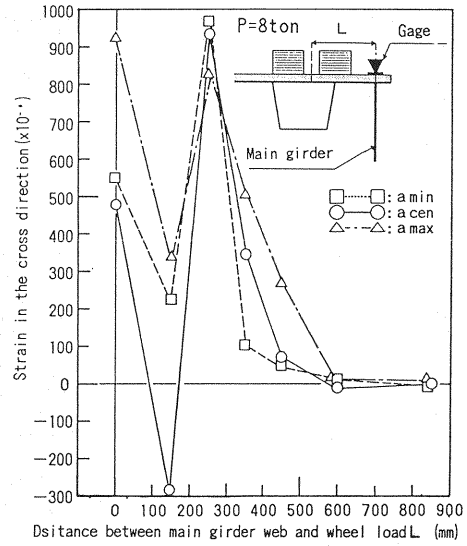


Fig.5 Effect of wheel position on the strain of the top surface of the pavement.

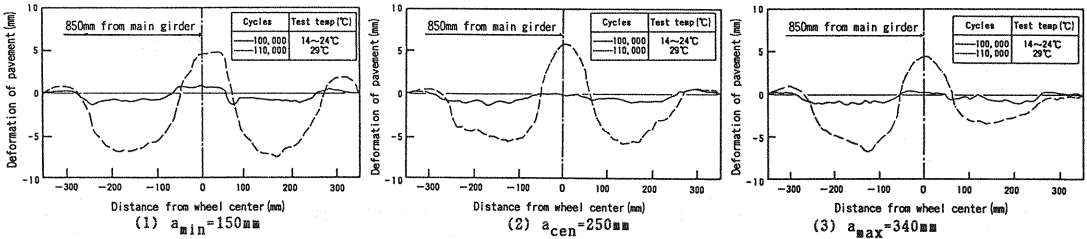


Fig.6 Deformation of the pavement ( $L=850$  mm).

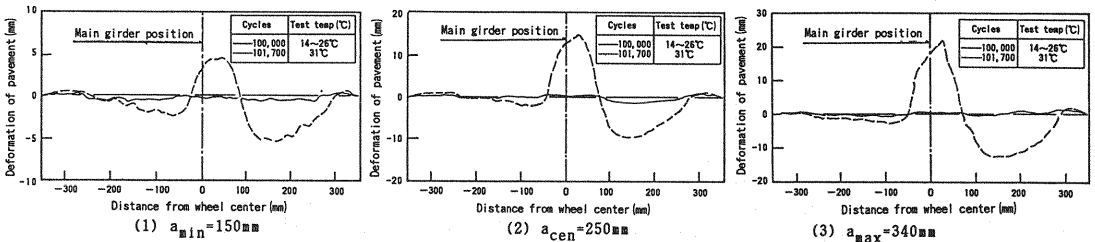


Fig.7 Deformation of the pavement ( $L=0$  mm).

(ton). Fig.5 shows the effect of the wheel positions on the strain of the top surface of pavement.

The strain of the top surface of the deck plate increases as the wheel load position nears the main girder web. In the case of  $a_1=a_{\min}$ , the strain increases almost uniformly while in the cases of  $a_1=a_{\text{cen}}$  and  $a_1=a_{\max}$ , it increases unevenly. Presumably, due to additional local displacement generated between the main girder web and the longitudinal rib as one of the double wheel is positioned between the main girder web and the longitudinal rib.

On the other hand, the strain of the top surface

of the pavement differs according to the wheel position, i.e. in the case of  $L \geq 600$  mm, no strain occurs. While in the case of  $600 \text{ mm} > L \geq 350$  mm, the greater the  $a_1$ , the greater the strain, and there is no strain tendency when  $250 \text{ mm} > L > 0$  mm. This is because while in the case of  $L \geq 350$  mm the wheel load is not positioned on the measuring point, in the case of  $250 \text{ mm} \leq L > 0$  mm, it is positioned directly on the measured point, and in the case of  $L=0$  mm, it is positioned on the clearance between the double wheels.

Fig.6 and Fig.7 show the measured results of pavement deformation (amount of surface irregu-

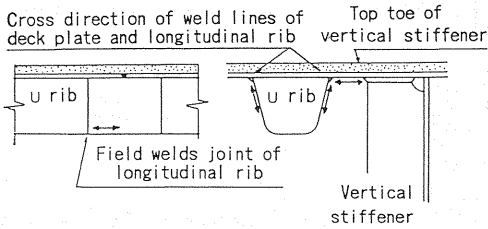


Fig.8 The object of analysis.

larity) at the center of the longitudinal rib span after repeated loading. The pavement surface either indicated little deformation at the normal temperature. And no pavement crack occurred during the first 100 000 cycles of repeated loading. As this could be due to the fact that the cycles of repeated loading were insufficient, and that testing was performed at a low temperature, repeated loading was performed again after heating the pavement. Both figures also show these additional test results.

Static loading tests performed after repeated loading indicated no distinctive difference in the behavior of the strain in the details of steel deck plate before repeated loading. The pavement deformation at the loading position  $L=850$  mm was minimal, and no significant difference due to  $a_1$  was observed. On the other hand, the pavement deformation at the loading position  $L=0$  mm indicated no significant difference during the first 100 000 cycles of repeated loading. But in case of heating, the behavior of pavement deformation varied due to a difference of  $a_1$ . Crackings caused by the pavement deformation directly on the main girder web (between the double wheels) was first generated at  $a_1=a_{\max}$ . At the final stage of testing, in the case of  $a_1=a_{\max}$ , cracks were also generated at the outer side line of the double wheels.

The results of loading tests abovementioned suggest that the vehicle traveling position should preferably be as distant as possible from the main girder web. In this case,  $a_1$  in excess of 250 mm (the maximum value called by the HEPC Design Guideline) would not affect the pavement with regard to its deterioration. On the contrary, when the wheel position is directly on or near the main girder web, it is preferable to make  $a_1$  as narrow as possible to ensure a reduction in local deformation between the main girder web and the longitudinal rib.

## 5. EFFECTS OF WHEEL LOAD POSITION AND LONGITUDINAL RIB ARRANGEMENT ON FATIGUE OF ORTHOTROPIC STEEL DECK DETAILS

Fig.8 shows the three positions where the fatigue

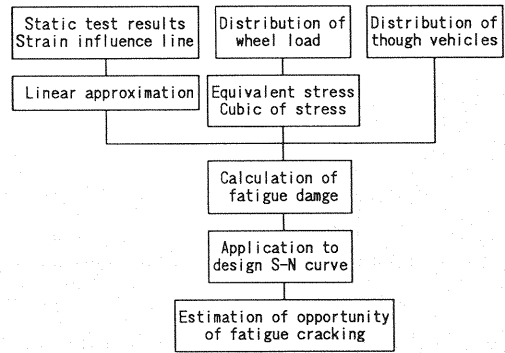


Fig.9 Flow chart of analysis.

cracks may be occurred. The effect of  $a_1$  on the fatigue damage of those based on the test results shall be investigated. Fig.9 shows the flow chart of analysis.

Generally when studying the fatigue of the structural details of the orthotropic steel deck, it is necessary to consider the stress influence line in the cross direction taking into account the area subjected to loading, the stress influence line in the longitudinal direction taking into the wheel load spacing and the traveling car spacing, and the design  $S-N$  curve of details.

Each factors shall be considered as follows :

The effect of  $a_1$  and  $L$  on the fatigue life ratio of calculated value to standard wheel position (See Fig.19) were investigated instead of the fatigue life. Because the fatigue life shall be affected with the asphalt deterioration and the increase of live load frequency.

One time of the fatigue damage is given by a wheel load. Therefore the tandem wheel is divided into two times of wheel load. The wheel loads used for analysis show Table 2.

The stress influence line in the cross direction shall be used the measured results.

The distribution of positions of traveling vehicles (See Fig.10) were used as the wheel traveling positions<sup>14)</sup>. The  $S-N$  curve was assumed as "stress<sup>3</sup>  $\times N = \text{Constant}$ " having no limit of the fatigue.

The following explains the analysis results.

Fig.11 shows the strain influence lines in the cross direction near the bottom of longitudinal rib. Increasing  $a_1$ , the strain on the main girder side also increases. Compared with the FSM analysis results, the measured values are small at most points, presumably due to errors in the analysis methods, and mainly due to the influence of the effectiveness of load distribution due to the pavement.

Fig.12 shows the calculated results of the fatigue life ratio. The fatigue life on the main girder side of  $a_1=a_{\min}$  and  $a_1=a_{\text{cen}}$  becomes greater in length

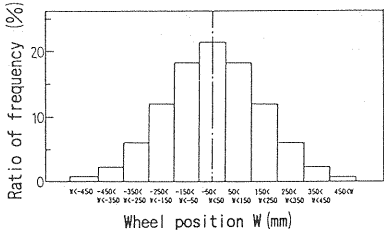


Fig.10 Distribution of position of traveling vehicles.

Table 2 Model live load.

Wheel type No	Composition Ratio (%)	Distribution model types*	Average load	Standard diviation	Upper limit (ton)	Lower limit	Equivalent load**
1	1.117	2	2.36	0.8	6.15	0.95	3.09418
2	0.582	1	2.09	0.5	4.2	0.8	4.18527
3	0.508	2	4.68	1.0	6.0	2.1	4.84135
4	0.027	3	6.85	0.8	14.0	6.0	7.53683
5	3.422	2	2.9	0.5	5.4	1.15	3.4982
6	1.102	1	2.41	0.4	3.68	0.98	3.67853
7	1.102	1	1.42	0.2	2.17	0.57	2.16926
8	1.975	2	5.29	0.8	6.93	2.24	5.71112
9	1.975	2	3.11	0.5	4.07	1.31	3.54993
10	0.027	3	7.66	0.7	5.74	6.93	8.29318
11	0.027	3	4.51	0.4	9.26	4.07	5.21297
12	0.165	1	2.03	0.3	2.9	0.77	2.89501
13	0.165	1	2.03	0.3	2.9	0.77	2.89501
14	0.154	2	4.4	1.0	12.5	1.85	5.11987
15	0.154	2	4.4	1.0	12.5	1.85	5.11987
16	1.402	2	2.4	0.5	4.8	1.3	3.02199
17	1.402	2	2.4	0.5	4.8	1.3	3.02199
18	0.481	1	1.98	0.5	3.65	0.95	3.62335
19	0.921	2	4.79	1.0	9.7	1.95	5.5062
20	0.062	2	2.12	0.4	4.12	1.45	2.70344
21	0.062	2	1.25	0.2	2.43	0.85	1.9183
22	0.132	2	2.54	0.9	6.18	0.82	3.2915
23	0.132	2	2.54	0.9	6.18	0.82	3.2915
24	0.099	2	2.44	0.8	6.55	0.95	3.18194
25	0.099	2	3.1	1.5	11.05	0.55	4.23296
26	0.099	2	3.04	1.7	11.85	0.85	4.30259
27	0.701	2	2.47	0.3	4.55	1.95	3.03038
28	0.331	1	2.05	0.4	3.5	1.9	3.0118
29	0.369	2	4.89	1.1	10.45	2.1	5.62093
30	0.287	1	1.31	0.4	2.35	0.65	2.30381
31	0.287	1	1.31	0.4	2.35	0.65	2.30381
32	0.414	2	4.43	1.2	10.45	1.22	5.24228
33	0.414	2	4.43	1.2	10.45	1.22	5.24228
34	0.162	2	2.71	0.3	4.45	1.95	3.25015
35	0.189	1	2.05	0.4	2.83	0.65	2.77551
36	0.189	1	2.05	0.4	2.83	0.65	2.77551
37	0.139	2	5.28	1.3	12.28	1.8	6.10734
38	0.139	2	5.28	1.3	12.28	1.8	6.10734

\* :Distribution type, 1;Normal, 2;Log normal, 3;exponent  
\*\* :Equivalent load; Cubic wheel load

with increasing  $L$ , and that on all other sides becomes shorter with increasing  $a_1$  and  $L$ , with little change. In particular, the fatigue life is almost identical at  $600\text{ mm} \geq L \geq 350\text{ mm}$ .

Fig.13 shows the strain influence line on the top of the vertical stiffener, and Fig.14 shows the calculated results of the fatigue life ratio. The strain in the top of vertical stiffeners are affected by the loading position, and the greatest value is indicated where one of the double wheels positioned on the top of a vertical stiffener. In addition, the narrower the  $a_1$  the greater the generating stress. The fatigue

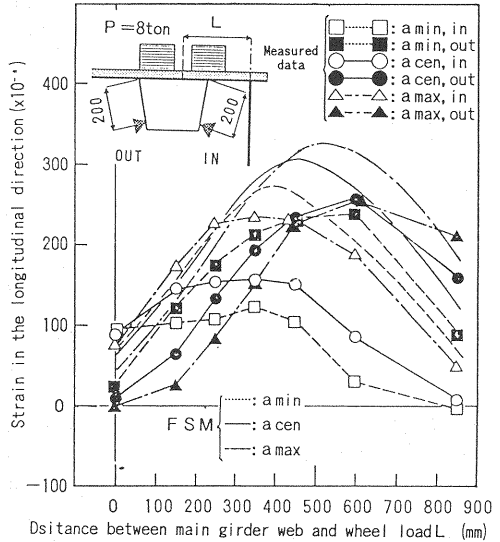


Fig.11 Effect of wheel position on the strain of the bottom of longitudinal rib.

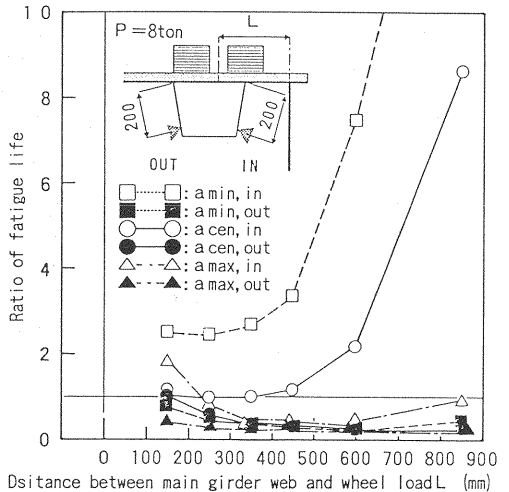


Fig.12 Effect of wheel position on the fatigue life ratio of the bottom of longitudinal rib.

life ratio increases with increasing  $a_1$  and  $L$  in the range of  $L > 450\text{ mm}$ . But  $a_1 = a_{\min}$  is longer than  $a_1 = a_{\text{cen}}$ , particularly in the range of  $L > 600\text{ mm}$ . This could be due to the varying profile of the influence line. Also, after the completion of repeated loading tests, the fatigue tests were carried out using a servo jack type fatigue testing machine under the conditions given in Table 3, and before  $50 \times 10^4$  cycles of each test case, the fatigue cracks was occurred in the boxing-weld on top of the vertical stiffener. Fig.15 shows that upon  $250 \times 10^4$  cycles, a crack developed to a total length of approximately 40 mm. In consideration of shifting

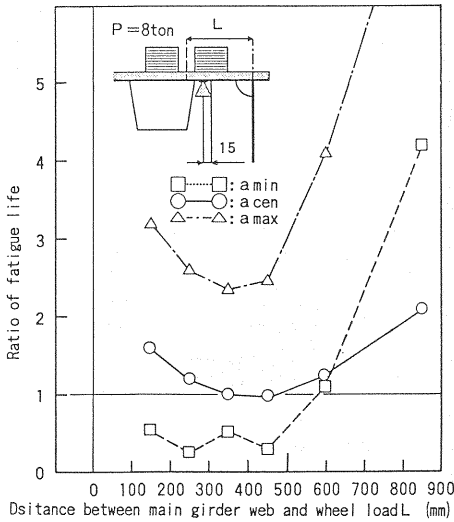


Fig.13 Effect of wheel position on the strain of the top of vertical stiffener.

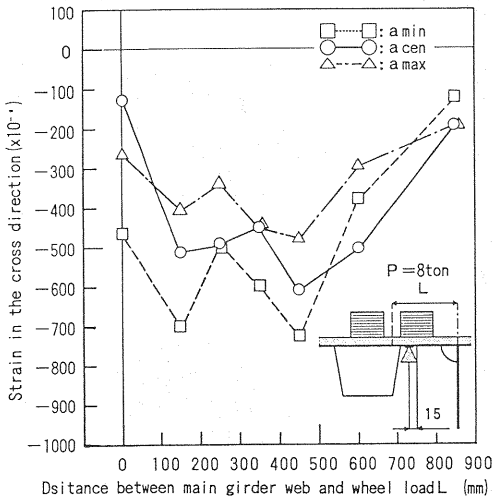


Fig.14 Effect of wheel position on the fatigue life ratio of the top of vertical stiffener.

and repeated wheel loads, the stationary development of this crack is not predictable.

Though the stress in the cross direction of the weld line in a U-shaped rib and deck plate does not need to be calculated in a general design works, the fatigue strength is very low, because the weld is a load carrying type one-side fillet weld. Though there has never been an instance of the fatigue damage to the abovementioned weld area in Japan, some fatigue damage directly beneath the wheel loads has been reported on Severn Bridge of the U.K. This is the reason that the probability of the fatigue crack shall be investigated. Fig.16 shows the influence line of the strain approximately 15 mm away from the weld toe, where the strain on

Table 3 Fatigue test case.

Test case	a, (mm)	Loading position	
		Longitudinal direction	Cross direction
1	a <sub>min</sub> (=150)	1/3 of longitudinal rib span	L=350mm
2	a <sub>cen</sub> (=250)		
3	a <sub>max</sub> (=340)		

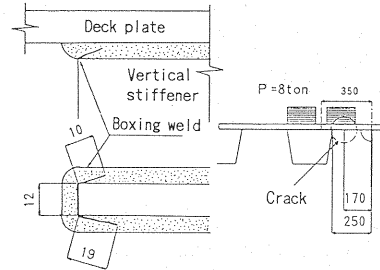


Fig.15 Example of fatigue crack.

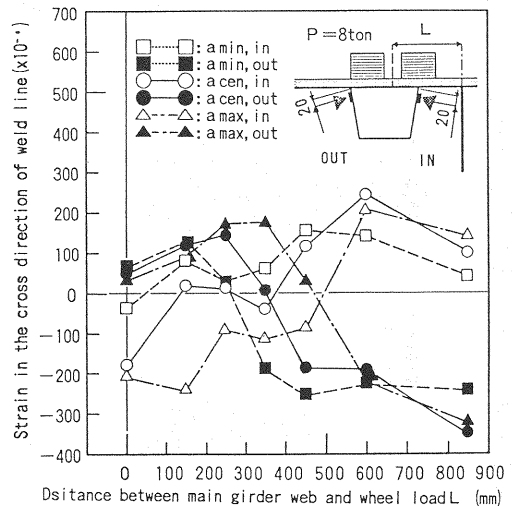
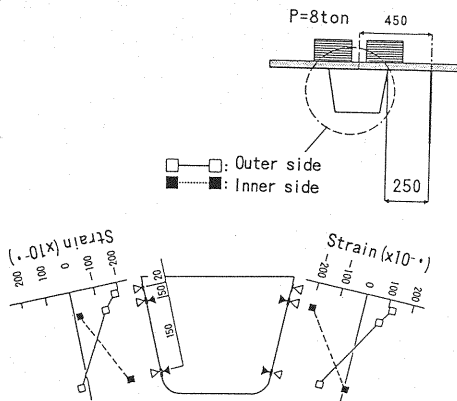


Fig.16 Effect of wheel position on the strain in the cross direction of weld line on the top of longitudinal rib.

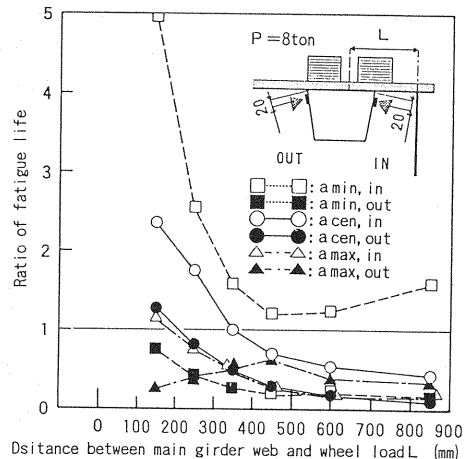
the right and the left of the ped rib indicates the behavior, with the positive and the negative almost reverse, regardless of the position of a wheel load. Also, from the example of strain distribution shown in Fig.17, the out-of-plane bending moments occur even with the wheel load directly on the plate.

Fig.18 shows the calculated results of the fatigue life ratio, where the smaller the  $a_1$ , the greater the difference of the fatigue life on the right and the left. When the outer side has a smaller fatigue life ratio,  $a_1$  causes a minimal change in the range of  $L > 450$  mm.

In addition, as a similar tendency was seen regarding the longitudinal ribs on the outer side,



**Fig.17** Example of the strain distribution in the height direction of longitudinal rib.



**Fig.18** Fatigue life ratio on the top of longitudinal rib.

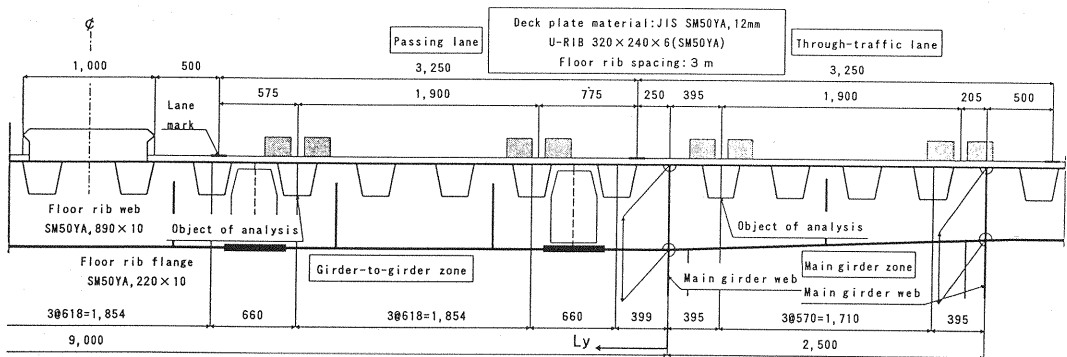


**Fig.19** Standard model bridge and its wheel load position.

the general longitudinal ribs positioned directly underneath the wheel load also presumably have a similar tendency due to their relations with the wheel load positions.

The results of loading tests abovementioned suggest that it is preferable to make  $L$  larger and  $a_1$  narrower in order to deal with the fatigue of the field joints of the longitudinal ribs and the welds in the longitudinal rib and the deck plate. On the other hand, for the top of the vertical stiffener, it became evident that  $L$  should preferably be larger as in the case of the abovementioned, but conversely  $a_1$  should preferably be larger. Thus, it would be preferable to make  $L$  larger and  $a_1$  narrower when considering the aspect of fatigue. In this case, however, it is necessary for the top of the vertical stiffener to be provided with a measure to locally improve the fatigue strength, such as by finishing the weld toes.

## 6. EXAMINATION OF THE OPTIMUM ARRANGEMENT OF LONGITUDINAL RIBS ON A STANDARD ORTHOTROPIC STEEL DECK

Through the results of the abovementioned loading tests, it is preferable for the traveling positions of vehicles to be separated (which means making  $L$  larger) from the main girder web.

However, this may involve difficulties due to road alignment and other factors, hence the effect of the spacing of longitudinal ribs on their stress shall be calculated using an actual model of a standard bridge.

The standard orthotropic steel deck used for analysis was that of a two-box girder bridge<sup>12)</sup> constructed of U-shaped ribs (hereinafter referred to as the “standard model bridge”). **Fig.19** shows its transverse section, and the positions of the wheel loads based on the results of a fact-finding survey on the actual line loads<sup>16)</sup>. For this standard model bridge, the analysis shall be used the orthotropic steel deck with five equidistant floor ribs and two floor beam, and was made using the



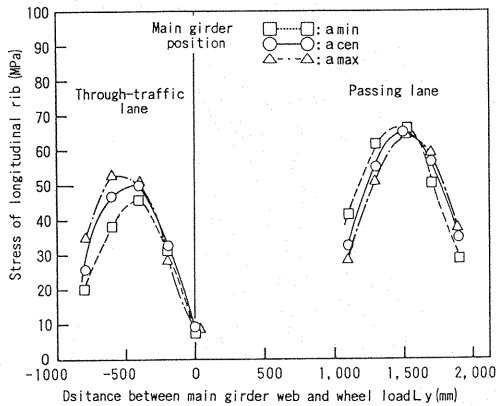


Fig.20 Analysis result.

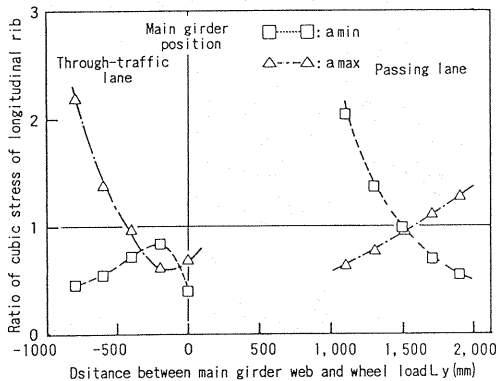


Fig.21 Cubic ratio of stress.

equivalent grille method. The superimposed load used was one T-20 load (not including the impact coefficient and the additional coefficient) in accordance with Section 6.2.2. of the Specifications for Highway Bridges.

Fig.20 shows the effects of the spacing of the main girder web and the longitudinal ribs on the stress acting in the center of the span of the longitudinal ribs positioned directly beneath the wheel load. While on the through-traffic lane the stress increases with increasing  $a_1$ , the stress on the passing lane differs in increasing and decreasing on the right and the left sides. Fig.21 shows the cubic ratio of longitudinal rib stress to the ratio of  $a_{cen}$ . Table 4 compares this with the ratio of the fatigue life derived in the same manner as in the case of Section 5, where the effect of narrowing the  $a_1$  on the orthotropic steel deck area within the main girder zone, is great. However, the reverse tendency is seen between the main girders, but with a minimal change.

## 7. CONCLUSIONS

In order to clear the effects of the spacing of the main girder webs and the longitudinal rib, and the

Table 4 Fatigue life ratio (%).

Main girder web and Longitudinal rib spacing $a_1$ (mm)	Through-traffic lane (Main girder zone)	Passing lane (Girder-to-girder zone)
$a_{min}$ (=150)	65.8	104.2
$a_{cen}$ (=250)	100.0	100.0
$a_{max}$ (=340)	115.0	95.8

positions of the wheel loads on the fatigue damage to the pavement laid on the main girder webs and to the welds of the orthotropic steel deck near the main girder web, the loading tests using a full-sized model with asphalt pavement have been carried out, thereby achieving the following results.

(1) The strain in the cross direction on the deck plate and the pavement directly on the main girder web differ according to the spacing of the main girder web and the longitudinal rib. In the distance between the main girder web and the wheel position  $L \geq 600$  mm, these strain is not affected by the spacing of the main girder web and the longitudinal rib.

(2) It is preferable to make the distance between the main girder web and the wheel position larger as well as the spacing of the main girder web and the longitudinal rib narrower, in order to prolong the fatigue life of the welds of the longitudinal ribs (which means the field joints and the welds between the deck plate and the longitudinal rib) positioned nearest the main girder web.

(3) To protect the top of the vertical stiffener from the fatigue damage, it is preferable for the distance between the main girder web and the wheel position to be larger as well as for the spacing of the main girder web and the longitudinal rib to be wider.

(4) When considering the fatigue of both the pavement and the steel members near the main girder web, it is preferable for the distance between the main girder web and the wheel position to be larger as well as for the spacing of the main girder web and the longitudinal rib to be narrower. In this case, it is necessary for the top of the vertical stiffener to be provided with a measure to improve the local fatigue strength.

(5) In case of the standard orthotropic steel deck two box girder bridge, it is preferable for the spacing of the main girder web and the longitudinal rib to be narrower. Because the position of the wheel load within main girder web directly underneath the travelling lane is close to the spacing between the main girder web and the longitudinal rib. On the other hand, in the girder-to-girder zone located directly beneath the passing

lane, it is feasible to widen the spacing of the main girder web and the longitudinal rib because wheel loads are not arranged near the main girder web.

### ACKNOWLEDGMENTS

The authors wish to acknowledge the members concerned of the Subcommittee for Steel Construction (headed by the late Dr. Akira Nishimura, Professor, Kobe University), the Deliberative Council, the Hanshin Expressway Public Corporation for their helpful guidance throughout the testing period, and to Dr. Toshio Horikawa, Assistant Professor and Dr. Akimitsu Kurita, Lecturer, both of the Osaka Institute of Technology, for their excellent cooperation in the carrying out of loading tests.

### REFERENCES

- 1) Public Works Institute : Design Handbook of Orthotropic Steel Deck, Public Works Institute data, No.399, July 1968.
- 2) Group for Investigation of Advancement in Bridge Deck Construction, Subcommittee for Investigation of Advancement, Committee of Steel Construction : Development and Status Quo of Steel Decks, Proceedings of the Japan Society of Civil Engineers, Vol.67.9, pp.34 ~ 40, Sept.1982.
- 3) Hoashi, Fukui and Asahi : Construction of Orthotropic Steel Deck Taking into Account its Pavement, the Bridges and Foundations, Feb.1980.
- 4) Honshu Shikoku Bridge Corporation : Design Guidelines for Orthotropic Steel Deck and its Commentary, Apr.1989.
- 5) Subcommittee of Orthotropic Steel Deck Fatigue, Committee of Steel Construction : Fatigue of Orthotropic Steel Deck, Proceedings of the Japan Society of Civil Engineers, No.410/I-12, pp.25~36, Oct.1989.
- 6) Tada : Practical Calculation Method for Orthotropic Steel Deck Using the Finite Strip Method, the Bridges and Foundations, Vol.5, May 1971.
- 7) Yamamura : Practical Calculation Method for Orthotropic Steel Deck with Closed Section (Trapezoidal) Type Ribs Using the equivalent grille method, the Bridges and Foundations, May 1981.
- 8) Public Works Institute : Fact-finding Results of the Pavement on Orthotropic Steel Deck, Public Works Institute data No.956, Mar.1974.
- 9) Iwasaki, Natori, Fukazawa and Terada : Examples of Fatigue Damage to Steel Bridges, and Measures for Repairing and Strengthening, the Technical Report of Yokogawa Bridge Works, Ltd. No.18, Jan.1989.
- 10) Kunihiro and Inoue : Applications of Fatigue Design to Orthotropic Steel Deck, Civil Engineering data, Feb.1972.
- 11) Japan Highway Association : Specifications for Highway Bridges and its Commentary, Feb.1980.
- 12) Hasegawa, Kondo, Yamada and Ishizaki : Verification of Fatigue of Box Girder Bridge's Orthotropic Steel Deck, Papers of Structural Engineering, Vol.35 A, Mar.1989.
- 13) Hanshin Expressway Public Corporation : Design Guidelines for Orthotropic Steel Deck, Feb.1989.
- 14) Hanshin Expressway Public Corporation : Investigations and Studies on Design Load System of Hanshin Expressways, Dec.1989.
- 15) Japan Highway Association : Design Guidelines for Highway Bridges and its Commentary, Feb.1988.
- 16) Okamura, Horikawa, Kurita and Matsui : Discussions on Self-propelled Type Wheel Tracking Testing Machine, Proceedings of Summaries of Lectures Delivered at the 43rd Annual Meeting of the Japan Society of Civil Engineers, PSI-2, Oct.1989.
- 17) Hanshin Expressway Public Corporation : Standard Drawings of Steel Structures, Oct.1989.

(Received March 26, 1991)